Supporting Material

Migration in confined 3D environments is determined by a combination of adhesiveness, nuclear volume, contractility, and cell stiffness

Lena A.Lautscham[1], Christoph Kämmerer[1], Janina R. Lange[1], Thorsten Kolb[1], Christoph Mark[1], Achim Schilling[1], Pamela L. Strissel[2], Reiner Strick[2], Caroline Gluth[1], Amy C. Rowat[3], Claus Metzner[1] and Ben Fabry[1]

[1]Biophysics Group, Department of Physics, University of Erlangen-Nuremberg, Erlangen, Germany

[2]Laboratory for Molecular Medicine, Department of Gynecology and Obstetrics, University-Clinic Erlangen, Erlangen, Germany

[3]Department of Integrative Biology and Physiology, UCLA, Los Angeles, USA

Supplementary Movie1: MDA-MB-231 cell with Hoechst-stained nucleus (red) migrating through the smallest (1.7µm wide) channel.

Supplementary Movie2: Overview of channel array with invading MDA-MB-231 breast carcinoma cells.

Supplementary Movie3: IFDUC1 breast cancer cells migrating through medium-sized channels (8.4-6.6 µm).

Supplementary Movie4: IFDUC1 breast cancer cells migrating through small channels (5.1-3.7 µm).

Cell culture:

All reagents were obtained from Gibco unless stated otherwise. MDA-MB-231 cells (obtained from ATCC) and A125 cells (gift from Peter Altevogt) are maintained at 37°C and 5% CO_2 in low glucose (1 g/L) Dulbecco's modified Eagle's medium supplemented with 10% fetal calf serum, 2 mM L-glutamine, and 100 U/ml penicillin-streptomycin. For lamin A transfected cells, 1 µg/ml puromycin is added to the medium. HT 1080 cells (obtained from ATCC) are maintained at 37°C and 5% CO_2 in advanced Dulbecco's modified Eagle's medium F-12 and supplemented with 5% fetal calf serum, 2 mM L-glutamine, and 100 U/ml penicillin-streptomycin. For lamin A transfected cells, 1 µg/ml puromycin is added to the medium. Primary breast cancer cells of mesenchymal origin

with high E-cadherin levels isolated from a patient with inflammatory duct (IFDUC1) breast cancer are maintained at 37°C and 5% CO_2 in collagen-coated dishes in Epicult-C medium (Stem Cell Technologies), supplemented with 1x Supplement C, 5% fetal calf serum, 2 mM L-glutamine, 50 U/ml penicillin-streptomycin and 0.5 mg/ml hydrocortisone (Stem Cell Technologies). Before plating, cells are rinsed with PBS and trypsinized with 0.05% trypsin/EDTA.

Soft lithography & PDMS device fabrication:

Channel devices are molded in polydimethylsiloxane rubber (Sylgard 184) from photolithographically developed masters (Fig. SI 1). AZ 15nXt photoresist (negative epoxy resin) (MicroChemicals) is diluted in 4 parts of AZ 1500 Thinner/PGMEA (MicroChemicals) and spin-coated onto 3'' silicon wafers at a spinning speed of 500 rpm for 15 s followed by 3000 rpm for 1 min, to form a resin layer of approximately 3.7 µm height. The coated waver is pre-baked for 1 min at 95°C followed by 2 min at 110°C. The photoresist is exposed for 14 s to UV light through a chrome mask with the help of a mask aligner. Post exposure bake is for 1 min at 95°C followed by 2 min at 110°C. Structures are developed using AZ 826 MIF (MicroChemicals). Hard bake is carried out for 10 min at 200°C. A second layer of resin is then applied to form the two square reservoirs flanking the channel array (Fig. 1A). For this, the channel structure is spin-coated again with AZ 125nXT at 1500 rpm for 2 s followed by 2000 rpm for 20 s. Pre-baking time for this resin is for 6 min at 140°C, and UV exposure time is 240 s through an acetate mask. No post-exposure bake is needed. The resin is developed with AZ 826 MIF and hard baked at 200°C for 10 min.

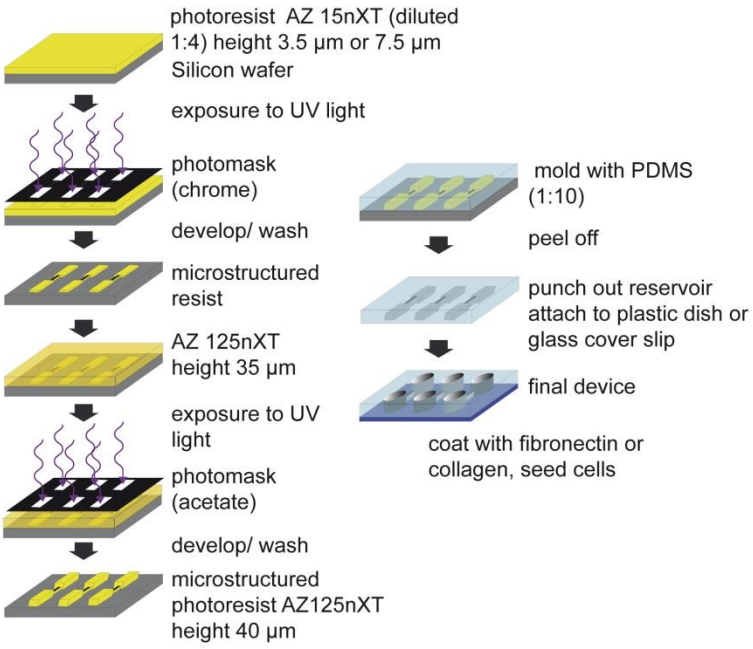

Figure SI 1: PDMS device fabrication

Each mask consists of 3 microarrays each with 10 lines consisting of 15 channels with decreasing width (11.2-1.7 µm diameter) separated by 20 × 20 µm chambers.

Devices are cast from polydimethylsiloxane with a 10:1 ratio of elastomer to curing agent, which is carefully mixed and degassed for 45 min at 0.2 kPa in a vacuum desiccator before pouring it onto the masters. After a curing time of at least 2 h at 65°C,

devices are peeled of the master, and reservoirs for holding the culture medium are punched, before bonding the devices to cell culture dishes (see Fig. SI 1, Fig. 1A).

Cell seeding:

PDMS devices are coated by adding 20 µl of 10 µg/ml fibronectin in PBS in each reservoir and sucking the solution into the channels by applying a vacuum of 5 kPa for 30 min. After incubation for 1 h at 37°C, the devices are washed twice with PBS. 3000 cells in 20 µl of cell culture medium are seeded in the reservoir located at the side of the larger channels. The other reservoir is filled with cell culture medium. After 4 h, both reservoirs are topped-up with cell culture medium, and the cell culture dish is filled with cell culture medium up to the height of the device. Cells are incubated for 1 week at 37°C and 5% CO_2 in the device before live cell image acquisition.

Live cell imaging and 2D cell migration tracking:

For measuring 2D cell migration, cells are plated 24 h prior to measurements on fibronectin-coated petri dishes. Cells are imaged with interference modulation contrast (IMC) using an inverted microscope (DMI6000B, Leica) and a 20x 0.4 NA objective with a 0.5x video coupler. Throughout the measurements, cells are kept in a custom-made incubation chamber at 37°C in humidified 5% CO_2 atmosphere. Images are taken every 300 s over a time period of up to 24 h. Cell movements are tracked with custom image processing software written in Matlab. From the cell trajectories, the mean squared displacement (MSD) is calculated as described in (1) and fitted with a power-law relationship of the form

$$MSD = D * (\Delta t / t_0)^{\beta} \qquad \text{(Eq. 1)}$$

with D denoting the apparent diffusivity (the MSD at the reference time t_0 = 1 min), and β denoting the power-law exponent. The time interval Δt ranges from 300s to 300 min. D characterizes the speed of cell movements at short time intervals, and β characterizes the persistence of cell movement at long time intervals (2). β typically ranges from a value of 1 for randomly migrating cells to a value of 2 for persistent, ballistically migrating cells (2). As D is log-normal distributed (2), the geometric mean and geometric standard error of D is computed.

Live cell imaging and 3D cell tracking:

For measuring cell migration in the channels, cells are monitored in interference modulation contrast (IMC) using an inverted microscope (DMI6000B, Leica) and a 20x 0.4 NA objective with a 0.5x video coupler. Throughout the measurements, cells are kept in a custom-made incubation chamber at 37°C in humidified 5% CO_2 atmosphere. Prior to imaging, cells are stained with Hoechst 33342 (Life technologies) at a concentration of 1.5 µg/ml. IMC images of the cells and fluorescence images of the

nucleus are obtained at a frame rate of 5 min. With a custom written Matlab software, the nucleus is detected by thresholding using Otsu's method, and the nucleus position and area are computed. The trajectories of the nuclei are transformed to the coordinate system of the microchannel array. The instantaneous nucleus speed is calculated as the change in position divided by the time interval between frames (5 min).

To obtain the average velocities of different cells as a function of the x-position, the velocity of each cell is linearly interpolated along the x axis. Furthermore, the velocity versus x-position data for each channel is divided into 3 binning regions and then averaged, namely the region left of the channel (entrance), the region inside the channel, and the region right of the channel (exit).

Bayesian Method of Parameter Inference:

From the nucleus trajectories, the time course of migratory persistence and activity is extracted with a Bayesian method of sequential inference (3, 4). This super-statistical approach describes heterogeneous random processes by a locally homogeneous model but allows the statistical parameters of the model to change with time. Statistical analysis of the extracted parameters then reveals subtle features of the random process that are not captured by conventional measures such as the mean squared displacement or the step width distribution.

From the measured positions x_t of the cell along the channel array, we compute a time series of steps $u_t = x_t - x_{t-1}$. Locally, this time series is modeled as an autoregressive process of first-order (AR-1), defined by $u_t = q_t\, u_{t-1} + a_t\, n_t$.

The parameter $q_t \in [-1,+1]$ describes the local persistence of the random walk, with $q_t = -1$ corresponding to anti-persistent motion, $q_t = 0$ to non-persistent diffusive motion, and $q_t = +1$ to persistent motion. The parameter $a_t \in [0, \infty]$ describes the local activity (noise amplitude) and sets the spatial scale of the random walk. Together, the two parameters determine the variance of the displacements according to $\mathrm{var}(u) = a_t^2 /(1-q_t^2)$. The quantity n_t is normally distributed, uncorrelated random noise with unit variance.

For constant parameters q_t and a_t, the AR-1 process is equivalent to a one-dimensional, persistent random walk. However, the spatially inhomogeneous environment of the channel array forces the cell to change its migration behavior as a function of time, which is reflected in time-dependent parameters q_t and a_t. We extract these time-varying statistical parameters from the measured time series $\{u_t\}$, using a Bayesian method of sequential inference (3, 4).

Live cell staining with Hoechst

To analyze deformations of the nucleus as the cells migrate through the channel system, the nucleus is stained with Hoechst 33342 (Life technologies). To find the best compromise between a bright staining contrast, low toxicity, and low exposure to UV light, we performed a series of experiments where we studied the influence of Hoechst concentration (0-25 µg/ml) and UV light intensity (0-10 mW/cm^2 every 5 min with a 500 ms exposure time) on the migration of cells on 2D substrates. To quantify cell migration, we measure the path length of the cells over a period of 6 h. Cell trajectories are obtained from interference modulation contrast images (IMC) recorded at a frame rate of 1 frame every 5 min. We find that HT 1080 cells and MDA-MB-231 cells respond to both UV light and Hoechst staining with a reduction of the migration path length (Fig. SI 2 A,B). We find a Hoechst 33342 concentration of 1.5 µg/ml and a UV light intensity of 7.2 mW/cm^2 to be an acceptable compromise between a good image contrast and low toxicity (<15% decline in migration).

We also measure the influence of staining with 1.5µg/ml Hoechst on cell stiffness in K562 cells using a microconstriction assay (5) and find that their stiffness increases by approximately 16% (Fig. SI 2 C). At the same time, these cells become more fluid like, as seen by the increase in the power-law exponent of the viscoelastic response by approximately 10% (Fig. SI 2 D).

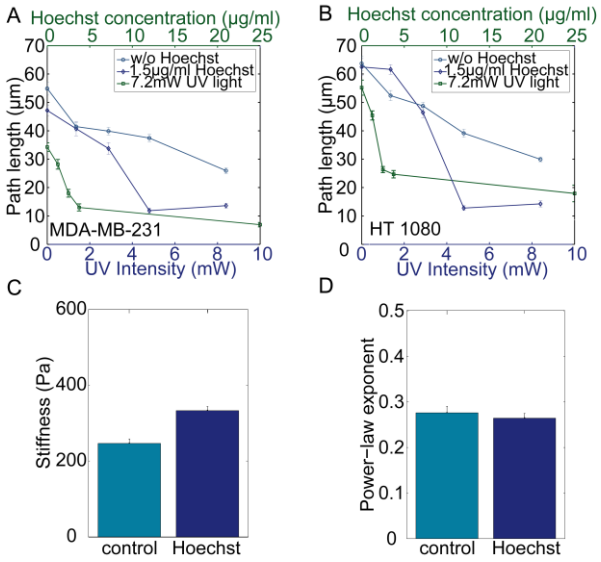

Figure SI 2: Influence of Hoechst staining and UV light intensity on cell migration in 2D for MDA-MB-231 breast carcinoma cells (**A**) and HT1080 fibrosarcoma cells (**B**). Path length of cells is measured over 6 h for different Hoechst concentrations and UV intensities. Light blue curve: Effect of different UV intensities on cells that have not been stained with Hoechst; Dark blue curve: Effect of different UV intensities on cells that have been stained with 1.5 µg/ml Hoechst; Green curve: Effect of different Hoechst concentrations at a constant UV light intensity of 7.2 mW/cm^2. (**C**) Cell stiffness of control and Hoechst treated K562 cells (mean ± se, n>2000 cells). (**D**) Power-law exponent of control and Hoechst treated K562 cells (mean ± se, n>2000 cells).

Traction microscopy:

Traction forces are computed from the displacements of beads embedded in a polyacrylamide gel with a Young's modulus of 11.3 kPa. Polyacrylamide gels are cast from a 40% acrylamide/bisacrylamide (ratio 37.5:1) solution (Sigma Aldrich). The solution is mixed with water to a final concentration of 6.1% acrylamide, and fluorescent beads are added. To initiate polymerization, 0.2% tetramethylendiamin (TEMED) and 0.5% amoniumpersulfat (APS) are added. Gels are functionalized using Sulfo SANPHA (Thermo Scientific). For cell type comparison, the gels are coated with 10 µg/ml fibronectin (15 µg/cm^2). To compare the influence of ligand density and ligand type, the gels are either coated with 0.5 µg/ml, 10 µg/ml, or 100 µg/ml fibronectin, or with 10 µg/ml collagen.

Cells are plated at a density of 1000 cells/cm^2 and incubated at 37°C and 5% CO_2 overnight. Throughout the measurements, cells are kept in a custom-made incubation chamber at 37°C in humidified 5% CO_2 atmosphere. A bright field image of the cell is taken to record the cell shape and position. Bead positions are recorded using fluorescence imaging. Subsequently, cells are relaxed or detached from the substrate by adding a 100 µl cocktail of 80 µM cytochalasin D and 0.25% trypsin in PBS. With no cell forces applied, the gel relaxes back to its stress-free configuration, and a second fluorescent image is taken. Bead displacements due to cell tractions are estimated with an unconstrained deconvolution algorithm, and cell tractions are computed using the Fourier transform traction cytometry method described in (6). From the displacement field and the traction force, we calculate the strain energy U according to (7) as

$$U = \tfrac{1}{2}\int(\text{Traction}*\text{displacement})\, dx\, dy \qquad \text{(Eq. 2).}$$

The cell contractility is then calculated from the traction force map by discretizing the applied forces on a grid. From this grid, the center of mass of the traction map is calculated. Subsequently, the force components pointing towards the center of mass are summed up, yielding the total contractility of the cell (8).

Lamin A lentiviral transduction:

For the generation of MDA-MB-231 and HT 1080 cells expressing eGFP-lamin A, lentiviral transduction is used. In brief, HEK293T cells are co-transfected with the vectors pMD2.G, psPAX2 and pLVX containing the coding sequence of lamin A N-terminally fused to eGFP using Lipofectamine LTX (Invitrogen). The cell culture supernatant is collected daily and replaced with fresh DMEM medium for the next 4 days. The collected medium containing assembled virus particles is pooled and filtered through 0.45 mm pores, supplemented with 8 mg/ml polybrene and added to MDA-MB-231 and HT1080 cells for 18 h. Starting from day 2 after lentiviral infection, cells are selected using 2.5 µg/ml puromycine.

Immunoblot analysis:

Cells are trypsinized, counted, and 10^7 cells are centrifuged and re-suspended in 100 µl PBS. 400 µl Laemmlie Buffer with 1 µl Benzonase Nuclease (Novagen) is added before heating the solution to 95°C for 5 min. Protein levels are tested with Pierce BCA (Thermo Scientific). Cell lysates are diluted to a protein concentration of 1500 µg/ml. Afterwards, the sample is diluted once more at 1:1 with Laemmlie Buffer containing bromphenol blue and 300 mM DTT (final concentration 150 mM), and heated again to 95°C for 5 min.

Individual protein fractions (20 µl) and molecular weight marker (10 µl) (PageRuler Prestained Protein Ladder, Thermo Fisher Scientific no 26616, Rockford USA) are subjected to SDS-polyacrylamide gel electrophoresis using 10% gels. Gels are electroblotted onto polyvinylidene difluoride membranes (Carl Roth) using a semi-dry transfer system with 25 mM sodium borate, pH 8.8, 1 mM EDTA as transfer buffer. Membranes are tested with the following primary antibodies: Anti-lamin A/C (LaZ) (clone #102 (9)) is diluted 1:5 , the polyclonal anti-LaA antibody (9), is diluted 1:50, the anti-β-actin antibody (Sigma, clone AC-15, cat. No A 5441) and anti-β-tubulin (Life Technologies, clone 2 28 33, cat. No 32-2600) are diluted 1: 2000. The secondary antibodies, peroxidase-coupled goat anti-rabbit immunoglobulin G and anti-mouse HRP (Invitrogen) are diluted 1:5000. All dilutions are in PBS and 0.05% Tween 20 with 5% milk powder at room temperature.

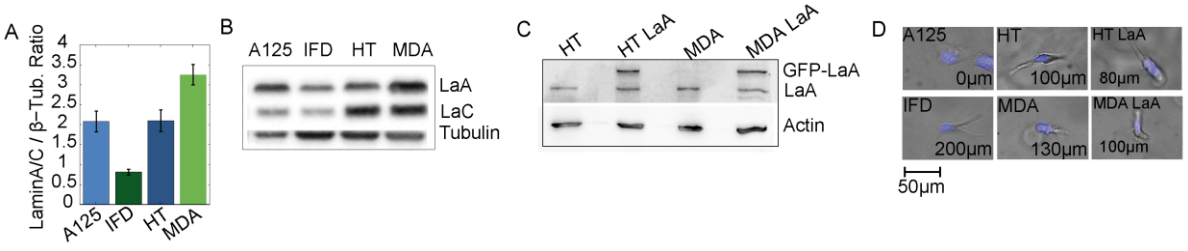

Figure SI 3: **A**) Lamin A/C expression levels in 4 cell lines normalized to β-tubulin (mean ± se of 3 independent experiments). (**B**) Corresponding western blot with antibody LaZ against lamin A/C. (**C**) Immunoblot showing lamin A and eGFP-lamin A expression level for control and lamin A overexpressing HT and MDA cell lines. (**D**) Representative images of cells that have invaded into a collagen gel (invasion depth as indicated) with Hoechst stained nucleus (blue).

Immunoblot analysis shows different indigenous lamin A/C levels for the four measured cell lines (Fig. SI 3 A, B). Wildtype cells and cells transduced with GFP-LaA show similar morphology and nuclear shape during invasion in a soft collagen gel (Fig. SI 3 D).

Adhesion strength assay

For evaluating the cell adhesion strength, a customized spinning disk device is used. The device consists of a rotating glass plate driven by compressed air. The glass plate is

located approximately 300 µm above a 35 mm plastic dish with adherent cells seeded at a density of 5000 cells/cm^2. The rotating plate generates a shear flow. Measurements are performed at a rotational speed of 1500 rpm, which results in an average shear stress of 32 dyn/cm^2 at a radial distance of 3 mm. The shear force is applied for 5 min to dishes coated with either 0.5 µg/ml, 10 µg/ml or 100 µg/ml fibronectin, or 10 µg/ml collagen. To compute the fraction of detached cells, the cell density at a radius of 3 mm around the center of the dish is measured before and after the application of the shear forces. For each condition, 3 independent experiments are performed.

Cell stiffness measurements:

For measurements of cell mechanical properties we use a microfluidic device consisting of a parallel array of micron-sized constrictions with a width of 5 µm and a height of 9 µm (5). Using a high-speed CCD camera, we measure the flow speed, cell deformation and transit time of several hundred cells per minute during their passage through the microconstriction array. From the flow speed and the occupation state of the constriction array with cells, the driving pressure across each constriction is continuously computed. We find that the transit time (t) decreases with increasing driving pressure (p) and decreasing cell radius (R_{cell}) according to a power-law.

$$t = t_0 * (\varepsilon E/\Delta p)^{1/\beta} \quad \text{with } \varepsilon = (\text{abs}((R_{eff}-R_{cell})/R_{cell}))^{1/2} \qquad \text{Eq. 4}$$

R_{eff} is the effective radius of the constriction (R_{eff} = 2.5µm). From this power-law relationship, the elastic (E) and dissipative properties (power-law exponent β = fluidity) of the cells are estimated.

Invasion Assay in a 3-D collagen gel:

2.4 mg/ml collagen gels are prepared by mixing 1.2 ml of collagen R (Serva, Heidelberg, Germany) with an equal amount (1.2 ml) of collagen G (Biochrom, Berlin, Germany), and adding 270 µl 10x DMEM (Biochrom), 270 µl $NaHCO_3$ (23 mg/ml stock solution) and 43 µl NaOH. 1.2 ml of the solution is polymerized for 2 h in a 35 mm dish at 37°C, 5% CO_2 and 95 % humidity. After 2 h, 2 ml of PBS are added. The following day, cells are seeded on top of the gel (5000 cells/cm^2) and are allowed to invade for 3 days. After 3 days, cells are fixed for 30 min with glutaraldehyde (2.5% in PBS) and stained for 30 min with 1 µg/ml Hoechst. The invasion profile is measured from optical sections obtained with a fluorescent microscope (10). The invasion profiles are plotted as cumulative probability of finding a cell at or below a given depth of the gel. The invasion profile is fitted with an exponential function, yielding the fraction of invaded cells as well as the characteristic invasion depth.

Cumulative probability analysis

We analyze the distribution of cell positions within the channels for the different cell types and take the slope of the cumulative probability as an indicator of relative migration velocity (and hence relative accumulation) in differently sized structures (Fig. SI 4 A). A125 cells show the steepest decline of the cumulative probability for channel sizes smaller than 5.4 µm, indicating that the migration of these cells is severely impeded. For HT cells, we find that the slope is steeper in the region with wider channels but then flattens out for channel sizes smaller than 5.4 µm. Hence, HT cells appear to accumulate in the narrow channels, indicating that they are able to migrate through narrow channels, albeit with a lower velocity. In the case of MDA and IFDUC1 cells, we find a nearly uniform distribution of cell positions, indicating that the average migration velocity is similar in all regions of varying channel widths. These data demonstrate that different cell lines respond differently to confinement.

To decipher the effects of increased cell stiffness on invasion, we analyze the distributions of cell positions within the channel array for eGFP-lamin A overexpressing cells and compare them with the distributions of non-transduced cells. We take the slope of the cumulative probability as an indicator of relative migration velocity and hence relative accumulation in differently sized structures (Fig. SI 4 B). We find a steeper decline in the probability of finding eGFP-lamin A expressing cells in channels with decreasing channel diameter.

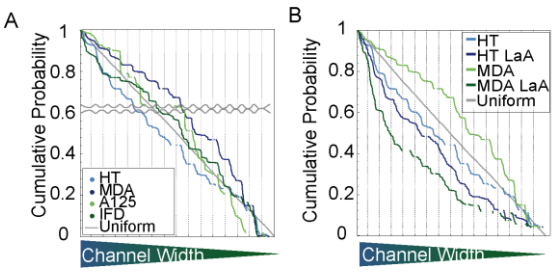

Figure SI 4: **A**) Cumulative probability of cell positions throughout channel structure. (**B**)) Cumulative probability of cell distribution throughout the channel array.

Nucleus shape analysis

We verify with confocal microscopy that the cross section of the nucleus fills the channel cross sections (Fig. SI 5). A channel-filling cross section of the nucleus for all channel sizes is also consistent with an analysis based on the known volume of the nucleus (measured from suspended cells), the 2D projected nucleus shape, and the height of the channel.

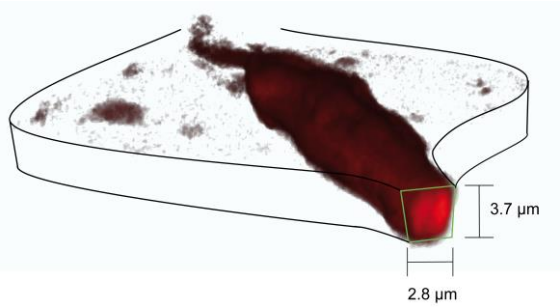

Figure SI 5: Confocal image stack of a cell moving from a chamber (black outline) into a 2.8 µm wide channel (cross-section in green). The cell nucleus is stained with Draq5 (dark red) and fills the cross-section of the channel.

Supporting References

1. Bursac, P., G. Lenormand, B. Fabry, M. Oliver, D. A. Weitz, V. Viasnoff, J. P. Butler, and J. J. Fredberg. 2005. Cytoskeletal remodelling and slow dynamics in the living cell. Nat Mater 4:557-561.
2. Raupach, C., D. P. Zitterbart, C. T. Mierke, C. Metzner, F. A. Muller, and B. Fabry. 2007. Stress fluctuations and motion of cytoskeletal-bound markers. Phys Rev E Stat Nonlin Soft Matter Phys 76 011918.
3. Mark, C., Metzner, C., Fabry, B. . 2014. Bayesian inference of time varying parameters in autoregressive processes. arXiv:1405.1668.
4. Metzner, C. M., Christoph; Steinwachs, Julian; Lautscham, Lena; Stadler, Franz; Fabry, Ben. 2015. Superstatistical analysis and modeling of heterogeneous random walks. Nature communications (under review).
5. Lange, J. R., J. Steinwachs, T. Kolb, L. A. Lautscham, H. I., G. Whyte, and B. Fabry. 2015. Microconstriction arrays for high-throughput quantitative measurements of cell mechanical properties. Biophys J in press.
6. Butler, J. P., I. M. Tolic-Norrelykke, B. Fabry, and J. J. Fredberg. 2002. Traction fields, moments, and strain energy that cells exert on their surroundings. American journal of physiology. Cell physiology 282:C595-605.
7. Koch, T. M., S. Muenster, N. Bonakdar, J. P. Buttler, and B. Fabry. 2012. 3D Traction Forces in Cancer Cell Invasion. PloS one 7:e33476.
8. Hersch, N., B. Wolters, G. Dreissen, R. Springer, N. Kirchgessner, R. Merkel, and B. Hoffmann. 2013. The constant beat: cardiomyocytes adapt their forces by equal contraction upon environmental stiffening. Biol Open 2:351-361.
9. Kolb, T., K. Maass, M. Hergt, U. Aebi, and H. Herrmann. 2011. Lamin A and lamin C form homodimers and coexist in higher complex forms both in the nucleoplasmic fraction and in the lamina of cultured human cells. Nucleus 2:425-433.
10. Mierke, C. T., B. Frey, M. Fellner, M. Herrmann, and B. Fabry. 2010. Integrin {alpha}5{beta}1 facilitates cancer cell invasion through enhanced contractile forces. J Cell Sci 124:369-383.